# Stress optical studies of oriented poly(methyl methacrylate)

**N. Kahar*, R. A. Duckett and I. M. Ward**
*Department of Physics, University of Leeds, Leeds LS2 9JT, UK*
*(Received 23 May 1977; revised 7 September 1977)*

A series of samples of oriented poly(methyl methacrylate) was produced by hydrostatic extrusion at temperatures below the glass transition temperature. The development of orientation in the process was monitored by the measurement of birefringence which was shown to depend on the extrusion temperature as well as on the applied deformation. Additional information to characterize the oriented state was obtained by measuring the shrinkage force which developed when the oriented sample, constrained to constant length, was heated to a temperature just above the glass transition temperature; specimens free to contract all recovered to the isotropic state and original dimensions on annealing at this temperature. Most measurements were made on specimens 'as extruded' with additional studies made on specimens annealed at temperatures above the extrusion temperature but below the glass transition. The data, which have strong implications with regard to deformation mechanisms, are interpreted both at a molecular level in terms of deviations from an ideal rubber network, and at a more phenomenological level in terms of the Mooney–Rivlin equation.

## INTRODUCTION

The research described in this paper forms part of a more extensive study of hydrostatic extrusion as a method of producing oriented polymers. Considerable attention has been given previously to crystalline polymers, where the aim has been to produce ultra-high modulus oriented materials[1]. Poly(methyl methacrylate) (PMMA) was chosen for this work as an example of an amorphous polymer, partly because isotropic cast sheet is readily available from commercial sources and partly because of our interest in the mechanism of deformation and the relationship between molecular orientation and imposed deformation. In the latter respect, previous studies of molecular orientation in PMMA using broad-line nuclear magnetic resonance[2] and laser-Raman spectroscopy[3] were expected to provide preliminary guidelines which would be of assistance.

In the present paper we will be concerned with the use of birefringence and shrinkage force as methods of characterizing the extruded samples. The measurements of birefringence relate to and extend previous studies of the development of birefringence in PMMA as a function of strain in plane strain compression, by Raha and Bowden[4]. It was clear from the latter work that the use of birefringence as a measure of molecular orientation is fraught with interpretative difficulties. This is even more true if one seeks to use birefringence as a tool to characterize a possible molecular network. For this reason we have followed previous research[5] on poly(ethylene terephthalate) (PET) and determined shrinkage force as an additional measure of the structure produced by deformation. This combination of birefringence and shrinkage force measurements links with previous stress optical studies on PMMA undertaken on samples deformed in a much higher temperature range, by Shishkin and Milagin[6].

* Present address: National Institute of Physics, JL. Cisitu 21/154D, Bandung, Indonesia.

It will be shown that such measurements on an extensive series of oriented samples prepared by extrusion at different temperatures, in some cases followed by annealing treatment, provide considerable insight into the mechanism of deformation.

## EXPERIMENTAL

### *Preparation of samples*

Uniaxially oriented rods of PMMA were produced by hydrostatic extrusion. The deformation was imposed by extruding PMMA rods through a die of exit diameter 0.7 cm. The nominal extrusion ratio (ratio of the final rod length to initial rod length) was determined by machining the rods to a given initial diameter. The pressure vessel containing the die was held at a fixed temperature, and extrusions were carried out at 50°, 90° and 100°C. A few additional extrusions were also made at 30°C. The highest nominal draw ratio which could be extruded successfully was 2.48. The hydrostatic pressures ranged up to about 1.5 kbar, and were applied using castor oil as the transmission fluid. Full details of the hydrostatic extrusion results, together with a detailed analysis of the mechanics of the process, are given elsewhere[7]. Particular points to note regarding the procedure were the use of molybdenum disulphide as a lubricant to reduce friction between the PMMA billet and the die, and the application of a small haul-off load to maintain a straight rod after extrusion. Swelling of the extrudate always occurred on leaving the die, reducing the maximum draw ratio achieved to about 2.0.

### *Thermal treatment of samples*

The first type of sample studied was the untreated extrudate. In this case, the isotropic PMMA billet was heated up to thermal equilibrium at the extrusion temperature and then extruded through the die at a relatively slow rate of deformation (strain rates $\sim 10^{-4}$–$10^{-3}$ $sec^{-1}$). On leaving

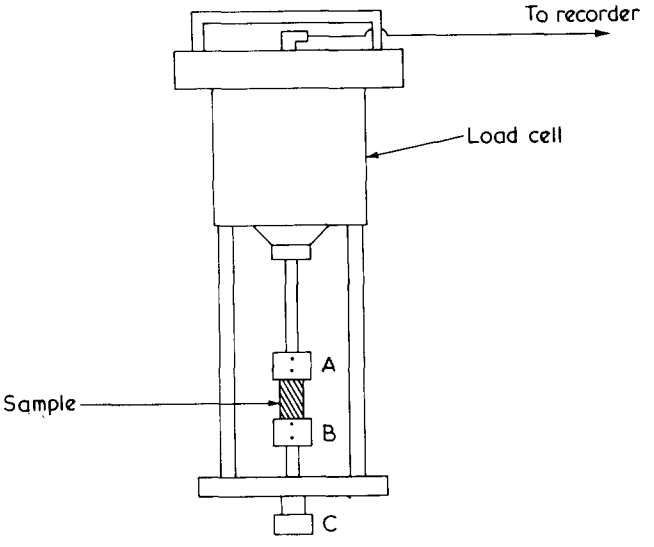


*Figure 1* Shrinkage force apparatus

the die the extrudate was allowed to cool rapidly to room temperature. For the different extrusion temperatures the extrusion conditions (haul-off load, extrusion speed, etc.) were made as close as possible for all draw ratios.

Two further series of samples were prepared from the initial extruded samples, first by annealing at constant length and secondly by annealing without constraint. Constant length annealing was carried out on thin sheets milled from the extruded rod, of length ~3 cm parallel to the extrusion direction. The sheets were held at constant length and immersed in a silicone oil bath at the annealing temperature. The time of annealing was chosen to be sufficient for the sample to reach its equilibrium state. It will be discussed below how this can be monitored by measurements of shrinkage force and birefringence. After annealing, the sample was removed from the oil bath and cooled to room temperature, still at constant length. Constant length annealing was undertaken at 116.5°C (above $T_g$) in conjunction with shrinkage force measurements, and also at lower temperatures, notably at 95°C.

Annealing of similar samples without constraint was carried out both above $T_g$, at 116.5° and 125°C, to test for recovery to the isotropic state, and at lower temperatures to produce anisotropic samples in a third well-defined manner.

*Measurement of the draw ratio*

As discussed above, the actual draw ratio (or extrusion ratio) of the extrudate is less than the nominal draw ratio. The actual draw ratios $\lambda$ for the extrudates were determined from the ratio of the initial cross-sectional area of the PMMA billet to its final extruded cross-sectional area, assuming that the volume remains constant. The final draw ratio $\lambda'$ for samples annealed without constraint was determined from the initial and final lengths of the sample parallel to the initial draw direction. The draw ratios calculated as above were also used to define the strain in the sample, $\epsilon = \lambda - 1$ and $\epsilon' = \lambda' - 1$ before and after shrinkage, respectively.

*Measurement of birefringence*

For birefringence measurement, a thin sheet of thickness 0.5–1.0 mm was milled from the extruded rod. The surface of the sheet was parallel to the axis of the rod, which is the draw direction. It was shown that variations in the milling conditions did not affect the resultant birefringence, which confirms previous findings by Haward and coworkers[8], who reported that the milling process does not alter the birefringence in PMMA.

The birefringences were measured in monochromatic light at 589 nm with a polarizing microscope, using an Ehringhaus rotary compensator. Most measurements were carried out at room temperature, and in a few cases birefringence was also measured at temperatures down to −60°C using a microscope cold-stage.

*Measurements of shrinkage force*

A schematic diagram of the apparatus constructed to measure the shrinkage force is shown in *Figure 1*. The sample milled from the extruded rod, with dimensions approximately 30 x 8 x 0.7 mm, the long axis parallel to the extrusion direction, is attached to an Instron load cell at one end A, and to a fixed metal grip B at the other end. The position of B can be altered by the screw C so as to set the sample just taut before heating. For the shrinkage force measurement the sample is immersed in a silicone oil bath, whose temperature can be controlled to ±0.1°C. The signal from the load cell is recorded on a chart recorder with two input channels, the second channel taking the signal from the thermocouple which monitors the temperature of the oil bath.

## RESULTS

*Birefringence measurements*

*Figure 2* shows the room temperature birefringence of the extruded samples as a function of the draw ratio. Also included are data for the samples annealed at constant length at 116.5°C. In general terms the results are similar to these obtained by Raha and Bowden for plane strain compression of PMMA in that the birefringence depends on both draw ratio and extrusion temperature $T_E$, although the data from 30° and 50°C extrusions superimpose. Full discussion of these results will be deferred until the shrinkage force data has been considered. The lines in *Figure 2* are fits to equation (2) as described in the Discussion section below.

Results of the low temperature birefringence measurements on selected samples are shown in *Figure 3* plotted in the form log $|\Delta n|$ vs. $T$, the temperature of measurement. The birefringence of all specimens was observed to change reversibly with temperature. The general form of the tem-

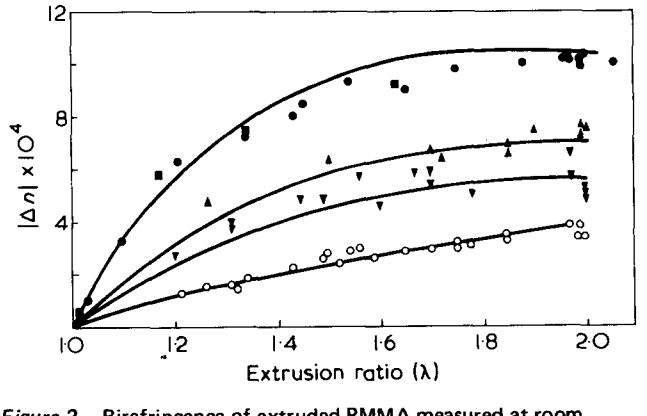


*Figure 2* Birefringence of extruded PMMA measured at room temperature. Extrusion temperatures; ■, 30°C; ●, 50°C; ▲, 90°C; ▼, 100°C. ○, represent the birefringence of samples of all extrusion temperatures after the shrinkage force measurement at 116.5°C, continuous curves from equation (2)

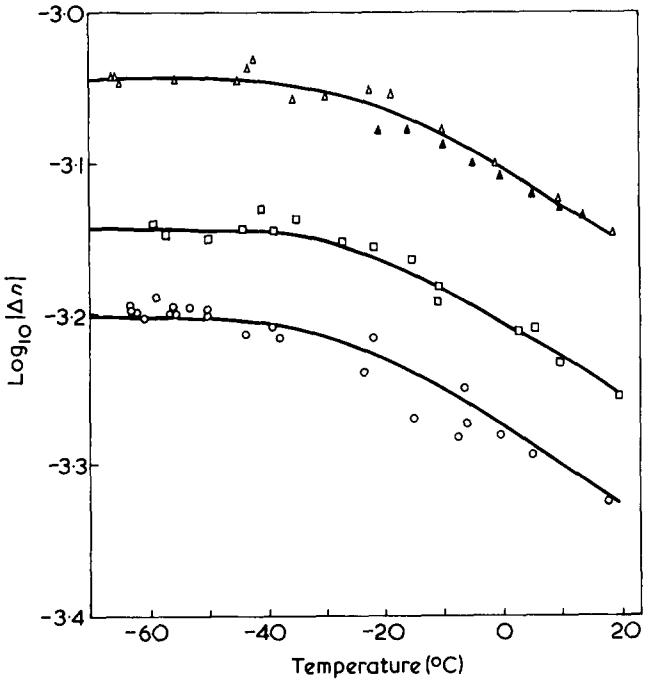


*Figure 3* The temperature dependence of the birefringence of extruded PMMA. ▲, $\lambda = 1.34$, $T_E = 50°C$; △, $\lambda = 1.93$, $T_E = 90°C$; □, $\lambda = 1.59$, $T_E = 90°C$; ○, $\lambda = 1.37$, $T_E = 90°C$

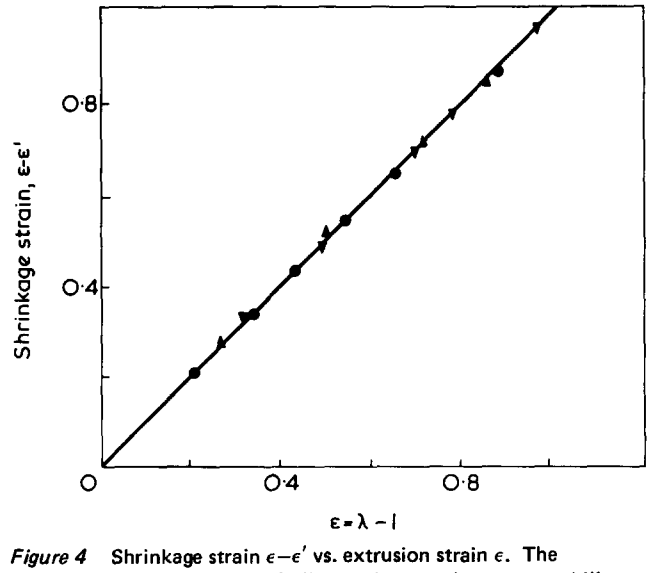


*Figure 4* Shrinkage strain $\epsilon - \epsilon'$ vs. extrusion strain $\epsilon$. The equality of these parameters indicates the complete recoverability of the deformation on annealing above the glass transition. ●, $T_E = 50°C$; ▲, $T_E = 90°C$; ▼, $T_E = 100°C$

perature dependence was similar for all specimens as shown in *Figure 3*. In particular the results from two specimens extruded to the same room temperature birefringence at different temperatures (50° and 90°C) are indistinguishable.

*Annealing without constraint above* $T_g$

Samples were annealed without constraint at 116.5° and 125°C for 30 min. The shrinkage strain $\epsilon - \epsilon'$ was then calculated from the length changes and compared with the actual draw ratio determined from the change in the cross-sectional area of the initial billet, as described above. The results are shown in *Figure 4*. No difference could be detected between results for two temperatures of annealing, nor were any further changes in length observed in samples annealed for 24 h. Complete recovery was achieved by annealing above $T_g$, as confirmed by the absence of birefringence in the annealed samples.

The relationship between residual strain and birefringence on annealing without constraint at 116.5°C shows remarkably similar behaviour for all materials tested. *Figure 5* shows data from three extrusion temperatures 50°, 90° and 110°C plotted in the form $\Delta n'/\Delta n$ *versus* $\epsilon'/\epsilon$ and all samples can be seen to follow a single curve. ($\Delta n'$ and $\epsilon'$ represent the current values of birefringence and sample strain during shrinkage of specimens extruded to the initial values $\Delta n$ and $\epsilon$, respectively.)

*Annealing without constraint below* $T_g$

Two methods for studying the free annealing (without constraint) were used. In the first experiment a single specimen was annealed for a fixed time (10 min) at each of a series of increasing temperatures 40°, 60°, 80°, 100°, 105°, 110° and 120°C. After each annealing period the specimen was cooled to room temperature to measure its birefringence $\Delta n'$ and dimensions before proceeding with the rest of the programme. In *Figures 6* and *7* the results

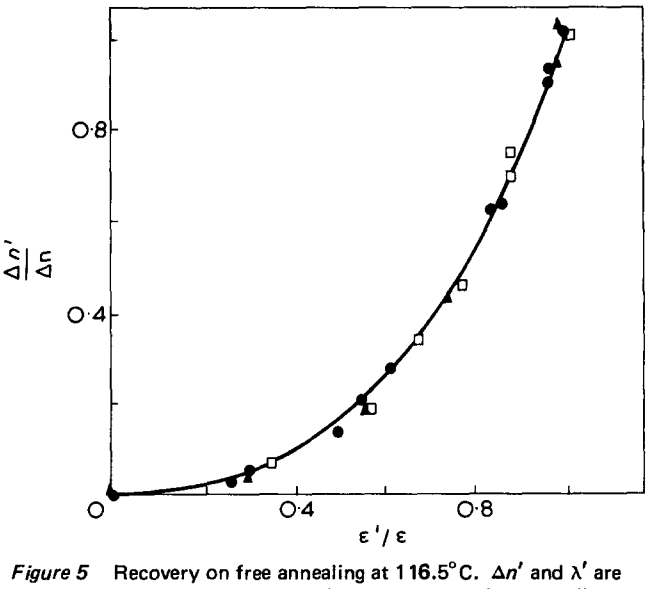


*Figure 5* Recovery on free annealing at 116.5°C. $\Delta n'$ and $\lambda'$ are the values of birefringence and deformation ratio after annealing of samples extruded to initial values $\Delta n$ and $\lambda$. ●, $T_E = 50°C$; ▲, $T_E = 90°C$; □, $T_E = 100°C$

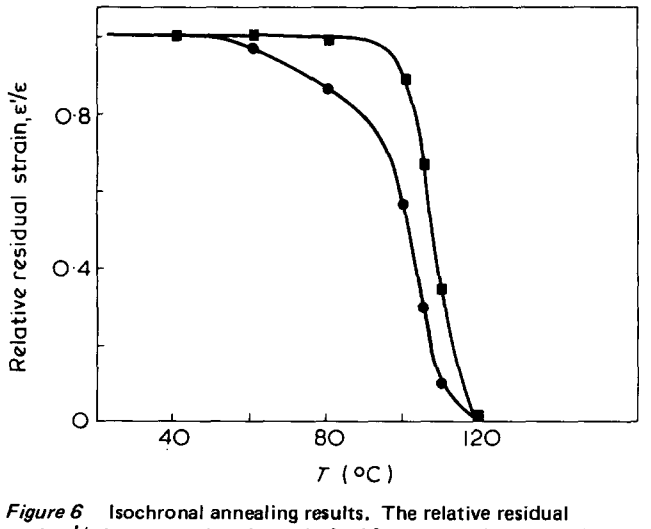


*Figure 6* Isochronal annealing results. The relative residual strain $\epsilon'/\epsilon$ is measured at the end of a 10 min period at each of the increasing temperatures 40°, 60°, 80°, 100°, 120°C. ●, $T_E = 50°C$; ■, $T_E = 90°C$

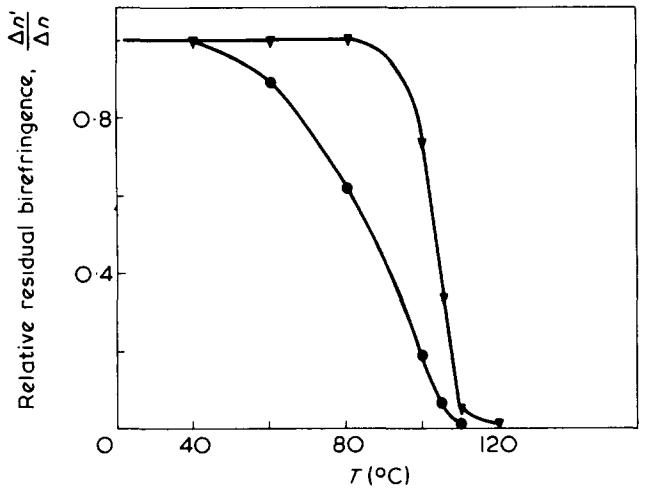


*Figure 7* Isochronal annealing results. The relative residual birefringence $\Delta n'/\Delta n$ is measured at the end of a 10 min period at each of the increasing temperatures 40°, 60°, 80°, 100°, 120°C. ●, $T_E$ = 50°C; ▼, $T_E$ = 90°C

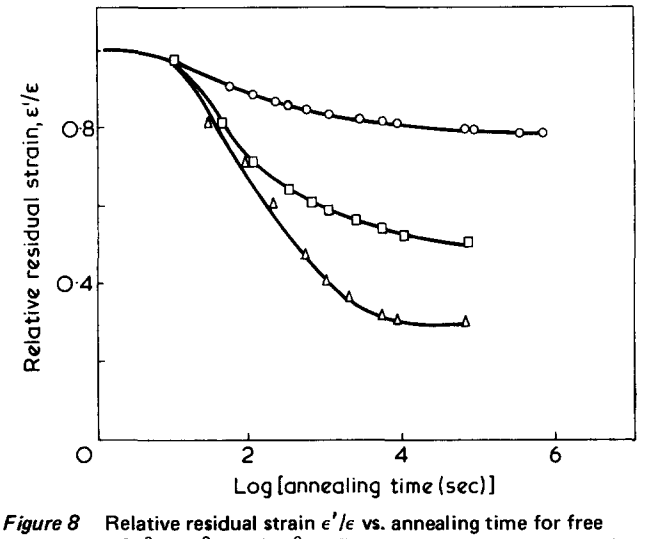


*Figure 8* Relative residual strain $\epsilon'/\epsilon$ vs. annealing time for free shrinkage at 80°, 100° and 105°C. The annealing was interrupted to monitor the residual strain and birefringence at various instants. Note that complete recovery is not reached even at the 105°C. The samples were taken from an extrudate with $\lambda$ = 1.99, $T_E$ = 50°C. Annealing temperature: ○, 80°C; □, 100°C; △, 105°C

are presented for annealing two samples ($\lambda$ = 1.96, $\Delta n = -10 \times 10^{-4}$, $T_E$ = 50°C and $\lambda$ = 1.97, $\Delta n = -5.6 \times 10^{-4}$, $T_E$ = 100°C) in the form of relative residual strain $\epsilon'/\epsilon$ and birefringence $\Delta n'/\Delta n$, respectively, *versus* temperature. The results show that appreciable shrinkage is observed at temperatures in the vicinity of and above the extrusion temperature, but that complete recovery is not achieved even at 105°C. These observations are confirmed by the results of the second method, shown in *Figures 8* and *9*, where the residual strain is plotted as a function of log (annealing time) for samples of the two extrudates featured in *Figures 6* and *7*, at each of the temperatures 80°, 100° and 105°C.

*Shrinkage force measurements*

As in previous work[5], the shrinkage force was measured as a function of time. In the first measurements to be considered the temperature was 116.5°C i.e. above $T_g$. Some key features of the behaviour are illustrated in *Figures 10* and *11*. First, in *Figure 10*, samples extruded to the same final draw ratio at different extrusion temperatures (50° and 100°C) are compared. Although the sample with the higher birefringence (extruded at the lower temperature) has the higher initial shrinkage force, the shrinkage force decays to a constant value which is identical for both samples. Secondly, it is interesting to make the opposite comparison, between samples extruded at different temperatures (50° and 90°C) to give the same birefringence. In this case there is a difference in draw ratio, the lower tem-

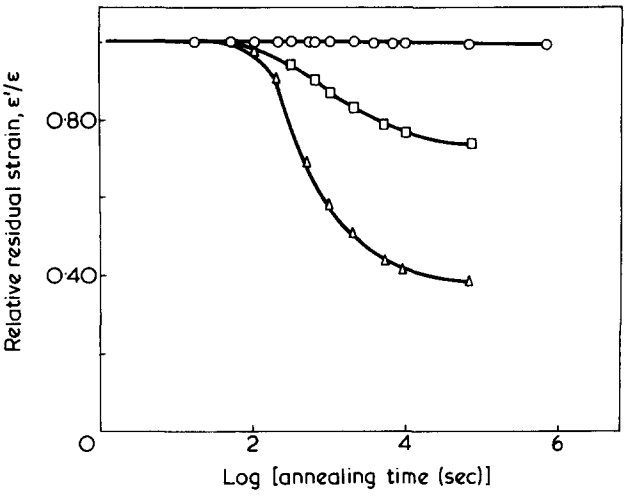


*Figure 9* Relative residual strain vs. annealing time, as for *Figure 8*. The samples were taken from an extrudate with $\lambda$ = 2.00 $T_E$ = 100°C. Note that recovery is negligible at temperatures below the extrusion temperature. Symbols as for *Figure 8*

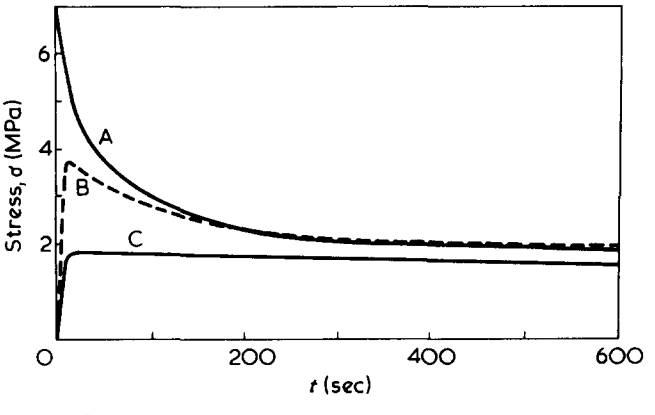


*Figure 10* Typical shrinkage stress curves on annealing at constant length at 116.5°C for specimens with the same extrusion ratio. Note the tendency of all three curves towards finite shrinkage stress at long times. A, $\lambda$ = 1.54, $T_E$ = 50°C; B, $\lambda$ = 1.56, $T_E$ = 100°C; C common curve for specimens as A and B, after heat treatment at constant length at 116.5°C until stress became constant

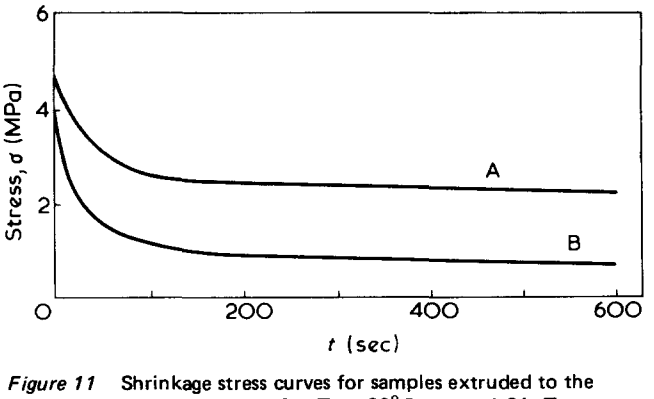


*Figure 11* Shrinkage stress curves for samples extruded to the same birefringence. A, $\lambda$ = 1.85, $T_E$ = 90°C; B, $\lambda$ = 1.21, $T_E$ = 50°C. Shrinkage at constant length at 116.5°C

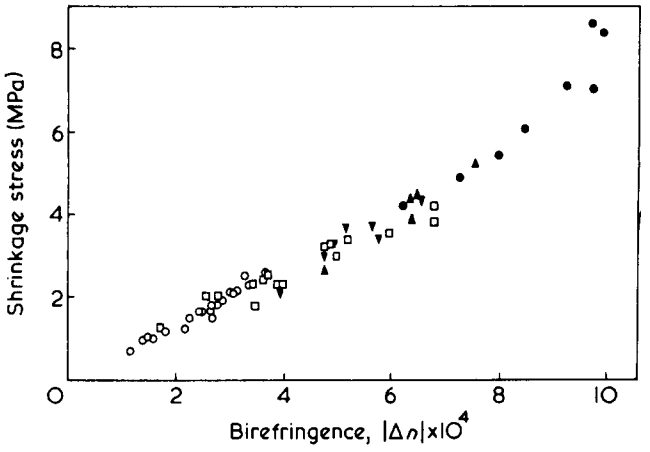


*Figure 12* Shrinkage stress *versus* birefringence for a range of samples. $T_E$: ●, 50°C; ▲, 90°C; ▼, 100°C; ○, 116.5°C; □, samples with various heat treatments, e.g. at constant length at temperatures below $T_g$ or after partial shrinkage at 116.5°C

perature extrusion sample having the lower draw ratio. In *Figure 11* it can be seen that the initial shrinkage force for the two samples is nearly identical, but that the final shrinkage forces are quite different.

These results taken together suggest the following. First, the peak shrinkage force is related to the birefringence of the extruded sample. Secondly, that the shrinkage force decays to a residual equilibrium value which is now related to the draw ratio imposed by extrusion and is independent of extrusion temperature.

The first of these conclusions is substantiated by a comparison of shrinkage force and birefringence for all extruded samples, together with those annealed at constant length in the shrinkage force experiment at 116.5°C. This comparison is shown in *Figure 12*, which confirms that there is a constant stress optical coefficient except for the highest values of birefringence where a slight increase is evident.

## DISCUSSION

### *Network theories*

The development of birefringence with strain for a rubber can be understood in terms of the Kuhn and Grün model of a network of flexible chains consisting of rotatable segments called random links[9]. For uniaxial deformation the birefringence $\Delta n$ is related to the extension ratio $\lambda$ by the equation:

$$\Delta n = \frac{2\pi}{45}\frac{(\bar{n}^2+2)^2}{\bar{n}} N\alpha(\lambda^2 - 1/\lambda) \qquad (1)$$

where, $\bar{n}$ is the mean refractive index of the network, $\alpha$ represents the difference in polarizabilities of the random link parallel and perpendicular to its axis and $N$ the number of chains per unit volume.

The curve for $\Delta n$ vs. $\lambda$ is characteristically convex towards the extension ratio axis (*Figure 13*) this equation holding in the so-called Gaussian approximation region, where affine deformation of the network junction points can be assumed. It has been found that the stretching of at least one amorphous polymer, PET, can be successfully modelled by this affine deformation scheme, both in the commercial spinning process[5] and in hot drawing at temperatures of ~80°C i.e. above the glass transition[10].

On the other hand, it is also well established that when PET is deformed *below* the glass transition (e.g. at room temperature) the birefringence/extension ratio curve is quite different and is now *concave* toward the extension ratio axis (*Figure 13*). It has been shown that the development of molecular orientation, measured by many techniques including birefringence, can then be modelled by assuming that the polymer consists of transversely isotropic units whose symmetry axes rotate on stretching in the same manner as lines joining pairs of points in the bulk material, which again deforms at constant volume[11]. This deformation scheme ignores the change in length of the units on deformation and considers only the rotational contribution. It has therefore been called 'pseudo-affine'[12].

It can be seen from comparison of *Figures 2* and *13* that the behaviour of PMMA is in some ways intermediate between these two deformation schemes*. Indeed the results for the development of birefringence on extrusion at 30° and 50°C are very reminiscent of similar data for PET, where below the glass transition the pseudo-affine deformation scheme holds at all temperatures[13,14]. In some recent papers it has indeed been suggested that a mixture of pseudo-affine and affine deformation occur. These papers include a study of molecular orientation in PVC by Maeda and coworkers[15] using polarized fluorescence, and neutron diffraction studies of polystyrene[16] where the authors refer to pseudo-affine deformation as 'uniformly affine'.

It is therefore of particular value to undertake measurements of shrinkage and shrinkage force since these provide information regarding a possible molecular network, separating this from the information on molecular orientation obtained from birefringence.

The complete recovery of the extruded PMMA samples to their original dimensions and zero birefringence on heating above $T_g$, does indeed suggest that the oriented glassy polymer can in all cases be considered as a deformed molecular network, irrespective of the details of the molecular

* Note the extended range of $\lambda$ ($\leqslant 4$) in *Figure 13* compared with *Figure 2*

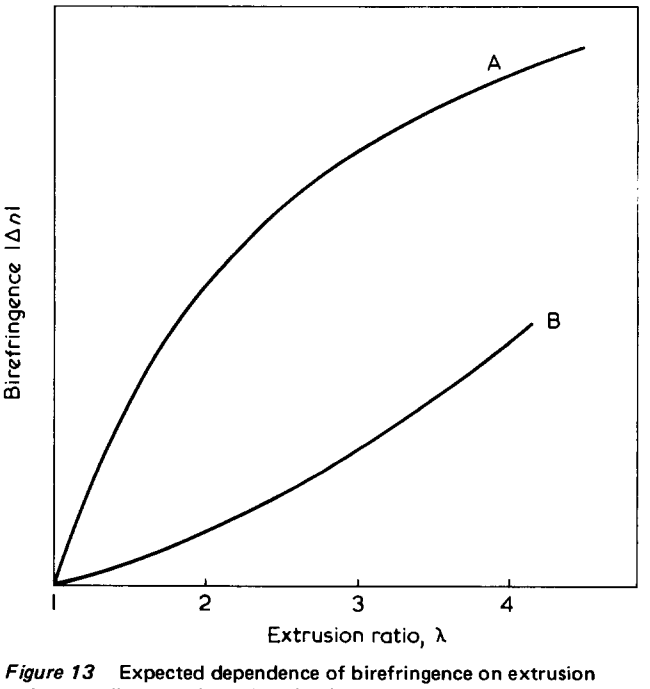


*Figure 13* Expected dependence of birefringence on extrusion ratio according to A 'pseudo affine'; B, rubberlike affine model deformation schemes

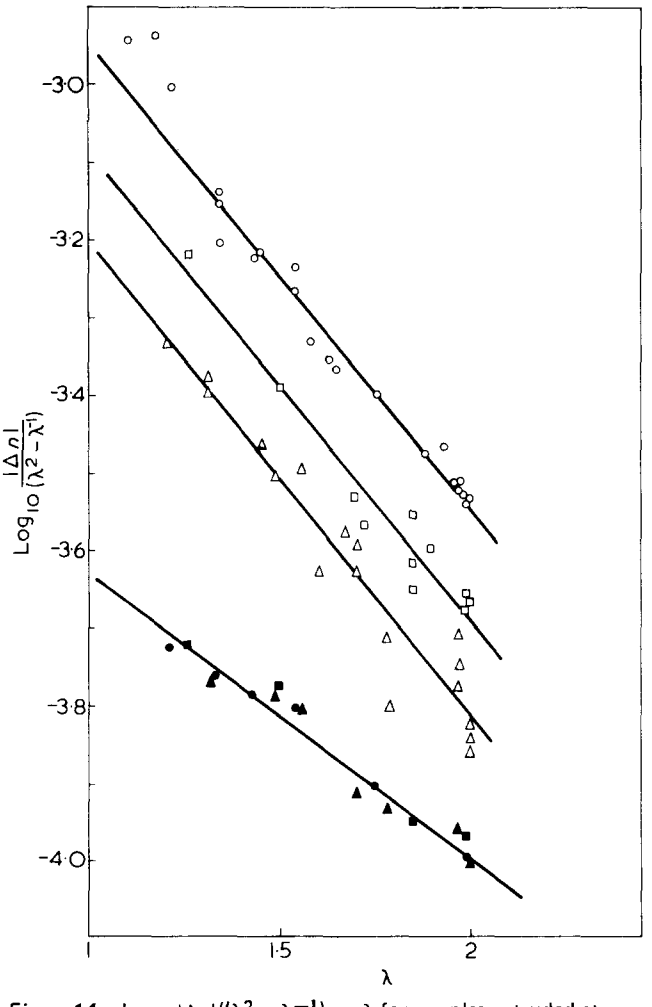


*Figure 14* $\text{Log}_{10}|\Delta n|/(\lambda^2 - \lambda^{-1})$ vs. λ for samples extruded at 50°C (○), 90°C (□), and 100°C (△). ●, ■, ▲, represent the residual birefringences of these samples after 10 min at constant length at 116.5°C

orientation. This network is 'frozen' in a strained configuration at room temperature, but on heating to temperatures above the extrusion temperature recovers some mobility, and in the absence ot external constraint shrinks back towards the isotropic unstrained state, annealing above $T_g$ producing complete recovery. The measurement of peak shrinkage force confirms the birefringence data in showing that the network deformation as well as the development of molecular orientation is not in accordance with the simplest molecular theory for the deformation of a rubber network.

Raha and Bowden[4] suggested that the development of birefringence in plane strain compression of PMMA could be described by the Kuhn and Grün model but adding the assumption that the network junction points were broken down with increasing strain. For a uniaxial deformation λ their theory gives:

$$\Delta n = CN_0\alpha(\lambda^2 - 1/\lambda)\exp(-k\lambda) \qquad (2)$$

where, $C = (2\pi/45)\,(\bar{n}^2 + 2)^2/\bar{n}$, $\bar{n}$ is the mean refractive index, $\alpha$ the difference in polarizabilities of the random link and $N_0 \exp(-k\lambda)$ represents the number of network junction points/unit volume in the strained state. $N_0$ is the number of junction points/unit volume in the unstrained state and was found by Raha and Bowden to depend strongly on the deformation temperature, whereas $k$ was an empirical constant approximately independent of temperature. In *Figure 14* data from the present work are plotted in the form of $\log(\Delta n)/(\lambda^2 - 1/\lambda)$ vs. λ and can be seen to confirm the general form of equation (2). This equation was used to construct the full curves in *Figure 2* using the values of $N_0$ and $k$ shown in *Table 1*†. The values of $N_0$ presented are in excellent agreement with those from Raha and Bowden, but small systematic differences are found between the values for $k$ between the results for extrusion and plane strain compression as might be expected from the differences in the nature of the deformation. As discussed by Raha and Bowden[4] and Shishkin and Milagin[6] the temperature dependence observed for $N_0$ is consistent with a cohesive energy of the junction points of 5–9 kcal/mol.

A very remarkable feature of the present study is the result that the peak shrinkage force from the extruded samples, measured at 116.5°C, is approximately proportional to the room temperature birefringence independent of deformation history. This suggests that despite the changes in the structure of the effective molecular network for deformation at different temperatures, there is nevertheless a constant stress optical coefficient. This is also true for samples which are subsequently heat treated, whether at constant length or free to relax. This result suggests that the nature of the 'random link' is unaffected by the deformation process or subsequent thermal history. Decreasing the temperature of deformation increases the number of network junction points $N_0$, and therefore only decreases the number of random links in each elemental chain of the network. The few results in *Figure 2* from extrusion at 30°C suggest that below 50°C no further increase in $N_0$ occurs and it appears that we are in a regime where the deformation no longer depends on temperature. In this regard the results are similar to the drawing of PET at low temperatures, and suggests that some of the ideas which have been used to describe the development of molecular orientation in PET[11] may prove to be of some relevance for PMMA. In particular, both in this work and in that of Raha and Bowden the development of birefringence at very low deformation ratios is more akin to the pseudo-affine deformation scheme.

Evidence for the nature of the random link itself comes from the absolute magnitude of the stress optical coefficient:

$$\frac{\Delta n}{\sigma} = \frac{2\pi}{45kT}\,\frac{(\bar{n}^2 + 2)^2}{\bar{n}}\,\alpha \qquad (3)$$

With reference to the current study, $\sigma$ in this equation represents the shrinkage stress measured at $T = 116.5$°C of a sample of birefringence $\Delta n$. From the room temperature

*Table 1* Parameters obtained from analysis of birefringence data in terms of equation (1)

| $T_E$ (°C) | $N_0 \times 10^{-26}$ ($m^{-3}$) | $k$ |
|---|---|---|
| 50.0 | 15.1 | 1.42 |
| 90.0 | 8.4 | 1.22 |
| 100.0 | 6.4 | 1.18 |
| 116.5 | 2.4 | 0.58 |

† The limited data from extrusion at 30°C do not appear significantly different from those at 50°C and can therefore be characterized by identical values of $N_0$ and $k$.

*Table 2* Model calculations for random link anisotropy in PMMA

| Anisotropy of link polarizability ($m^3$) | Conformations of $-COOCH_3$ group: *Trans* with respect to C–C and C–O | Free rotation about C–O trans C–C | Free rotation about C–O and C–C | Source (reference) |
|---|---|---|---|---|
| $(\alpha_{\parallel}-\alpha_{\perp}) \times 10^{31}$ | −18.2 | −15.3 | −1.87 | 18 |
| | −13.9 | −10.0 | 110.44 | 19 |

(20°C) birefringence data presented in *Figure 12* we obtain:

$$\frac{\Delta n_{20}}{\sigma} = -1.5 \times 10^{-10}\ m^2/N$$

By combining equations (3) and (4) and using $\bar{n} = 1.493$ we find that $\alpha_{20} = -4.8 \times 10^{-31}\ m^3$. This figure represents the polarizability difference of the random link at room temperature.

Examination of the birefringence data at low temperature in *Figure 3* reveals that the absolute value of the birefringence of any sample depends (reversibly) on the temperature of measurement. Furthermore, the observation that data from different temperatures can be superposed by a simple shift along the $\log(\Delta n)$ axis suggests that the form of the temperature dependence is identical for all samples, following the relationship:

$$\Delta n(T) = CN_0 \exp(-k\lambda)\,(\lambda^2 - 1/\lambda)\alpha(T) \qquad (5)$$

The temperature dependence of the birefringence of oriented PMMA and other polymers was observed by Andrews and Hammack[17]. They attributed the effect to the progressive quenching-out at decreasing temperatures of the $CH_3$ rotations on the pendant side groups. The birefringence measured at low temperatures must therefore be attributed to a 'frozen' network in which the random link anisotropy is numerically greater than at room temperature, and analysis of our data suggests that at −60°C:

$$\alpha_{-60} = -6.5 \times 10^{-31}\ m^3$$

It is helpful to compare the measured values of $\alpha$ with model calculations based on an assumed isotactic monomer conformation. These calculations[18,19] are very sensitive to details of the conformations and of the side-group rotations assumed, as shown in *Table 2*. Inspection of this Table shows that the measured values are consistent with a random link comparable with one monomer, birefringence measurements down to even lower temperatures would be necessary to confirm this statement.

The discussion so far has concentrated on analysis of the birefringence and shrinkage force data from the main extrudates. The data have been shown to be consistent with the concept of a frozen network with a junction point density dependent on extrusion temperature but with a constant random link. Further information is available from specimens which were heat-treated at temperatures above the extrusion temperature (but below $T_g$). It is very significant that again the shrinkage force on heating above $T_g$ and the final birefringence change is an exactly equivalent fashion. After sufficient annealing time the samples reach a new equilibrium state which is equivalent to extrusion to the same strain at the temperature of annealing (see *Figure 5*).

It is to be recalled (*Figures 10* and *11*) that on heating the extruded samples at constant length above $T_g$ the shrinkage force decays to a constant value which we believe reflects the existence of a 'permanent' network of molecular entanglements. The new equilibrium achieved by heating to a temperature below $T_g$ might therefore be attributed to a thermal breakdown of some temporary junction points (e.g. the electrostatic interaction crosslinks envisaged by Raha and Bowden[4]) to a level appropriate to the annealing temperature; this network of temporary junction points is augmented by the 'permanent' network of molecular entanglements. The exact correspondence between the changes in shrinkage force and birefringence is consistent with the view that a single mechanism, viz. the change in the total number of junction points in the network, is sufficient to explain the results.

We must also consider data from samples annealed without constraint above and below $T_g$. Annealing above $T_g$ results eventually in complete recovery of the isotropic state. Interruption of this process to measure the current values of birefringence $\Delta n$ and extension ratio $\lambda$, respectively, reveals that for all specimens independent of previous history the fractional residual birefringence $\Delta n'/\Delta n$ depends only on the relative residual strain $\epsilon'/\epsilon$ as shown in *Figure 5*.

Annealing below $T_g$ (but above the extrusion temperature) results in partial recovery, with samples following the 'trajectories' marked by broken lines in *Figure 15*. Again the samples reach a new equilibrium state, in this case with a new value of the extension ratio $\lambda'$. The new equilibrium is such that an annealed sample is equivalent in shrinkage force and birefringence to a sample which had been extruded to the final extension ratio $\lambda'$ at the annealing temperature.

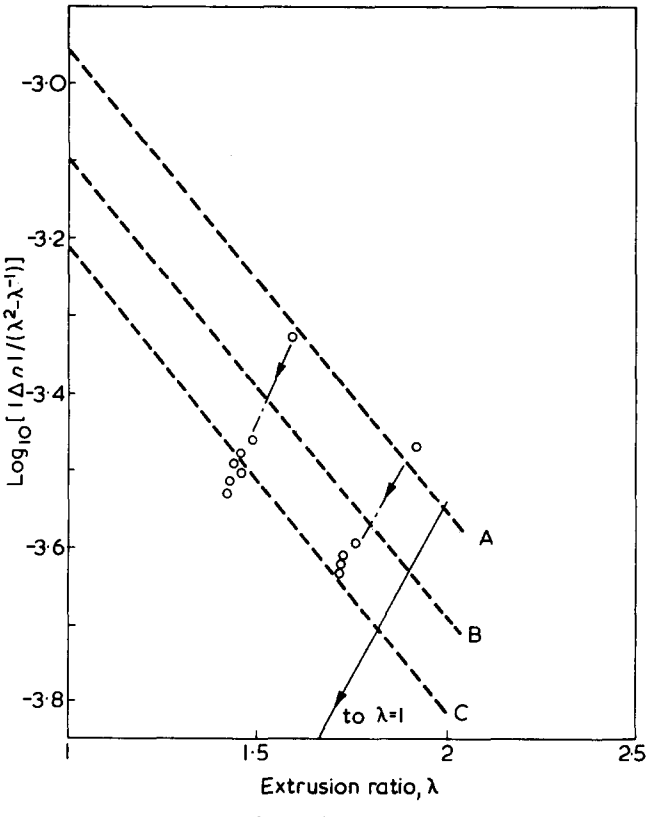


*Figure 15* $\text{Log}_{10}\,|\Delta n|/(\lambda^2 - \lambda^{-1})$ vs. $\lambda$. ○, Data from samples annealed free at 100°C. – – – –, represent data on 'as-extruded' samples (from *Figure 14*). ——, 'to $\lambda = 1$' shows the trajectory of a sample annealed free at 116.5°C (from *Figure 5*). Extrusion temperature: A, 50°C; B, 90°C; C, 100°C

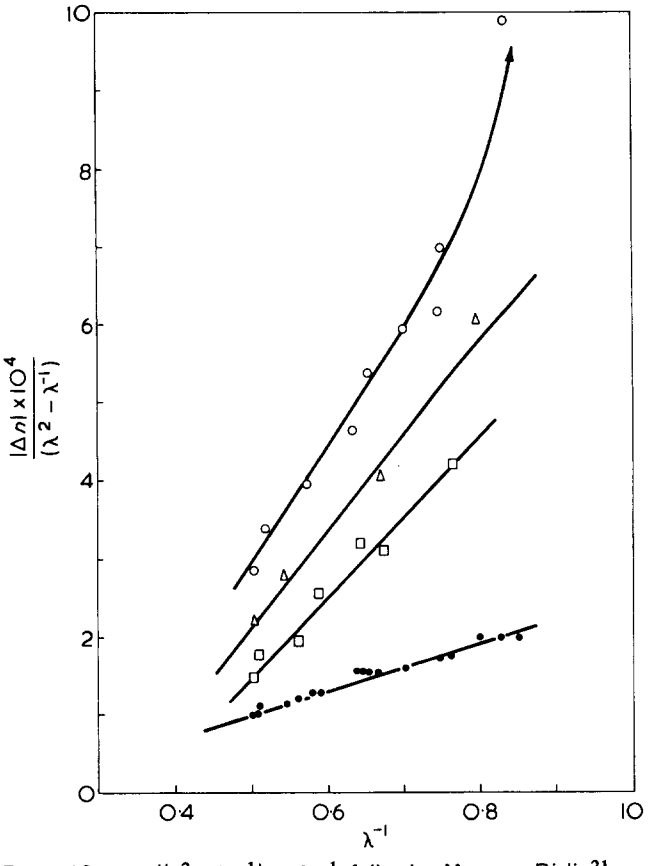


*Figure 16* $|\Delta n|/(\lambda^2 - \lambda^{-1})$ vs. $\lambda^{-1}$, following Mooney–Rivlin[21] and Saunders[22]. $T_E$ = ○, 50°C; △, 90°C; □, 100°C and ●, samples after annealing at constant length at 116.5°C

We have recently become aware of an independent study of the free shrinkage of oriented PMMA by Hennig[20] which suggests that the recovery can be considered as the sample 'creeping' towards the isotropic state; the entropic restoring forces are opposed by the time dependent creep modulus appropriate to the annealing temperature. (At temperatures below 50°C say the glassy modulus is high and so there is negligible shrinkage whereas at 116.5°C the glassy modulus is effectively zero and shrinkage is unimpeded.) This explanation is consistent with the present investigation and we can see that in a general sense our results conform. For example the degree of shrinkage (and rate of shrinkage) at a given temperature is related to the initial birefringence, which is proportional to the shrinkage force (*Figures 8* and *9*).

With these considerations we are now moving away from the ideas of Raha and Bowden in our interpretation of the term $\exp(-k\lambda)$ in equation (2). They suggested that this term arose from the breakdown of junction points during deformation and associated it with $N_0(T_E)$, the unstrained junction point density at the deformation temperature. This interpretation leads to difficulties when interpreting changes of deformation during shrinkage. There are also difficulties in understanding the relative independence of temperature of the parameter $k$ if it is supposed to model a specific molecular mechanism. We therefore propose that the term $\exp(-k\lambda)$ $(\lambda^2 - 1/\lambda)$ can be considered together as modelling the finite deformation of the network, which takes place at constant junction point density, $N_0(T_E)$. This essentially phenomenological interpretation is pursued further in the next section.

*Phenomenological approach*

We have just seen that the data presented here can be adequately represented by equation (2). There is however an alternative representation of the development of birefringence and shrinkage force with deformation. It is well known that the stress developed in a rubber can often be accurately described by the Mooney–Rivlin equation:

$$\sigma = 2(\lambda^2 - 1/\lambda)(C_1 + C_2/\lambda) \qquad (6)$$

where $C_1$ and $C_2$ are constants[21]. Saunders[22] has shown that a similar equation holds for the birefringence as a function of strain for elastomers. It is however not necessary (or even perhaps usual) for there to be a constant stress optical coefficient[23] as observed here for PMMA.

*Figure 16* shows the present results plotted in the form $\Delta n/(\lambda^2 - 1/\lambda)$ *versus* $1/\lambda$. It can be seen that this representation of the data is equally acceptable at a phenomenological level to that provided by equation (1). The physical interpretation of the deviation from the simple statistical relationship:

$$\Delta n = CN_0\alpha(\lambda^2 - 1/\lambda)$$

is however quite different from that proposed by Raha and Bowden[4]. We do not have to infer that there is a breakdown of network junction points during deformation. Rather the deviations are seen as a common feature for all rubber networks as emphasized in a recent review by Treloar[21].

In the original treatment due to Mooney the terms $C_1$ and $C_2$ are related to the stored energy $W$ and the strain invariants $I_1$ and $I_2$ through

$$C_1 = \left(\frac{\partial W}{\partial I_1}\right)_{I_2} \text{ and } C_2 = \left(\frac{\partial W}{\partial I_2}\right)_{I_1}$$

The Mooney theory requires that both $C_1$ and $C_2$ should be constant. In addition $C_1$ has frequently been identified with the entropic contribution to the modulus, as derived from the statistical theory of rubber elasticity. Treloar[21] points out that in general $(\partial W/\partial I_1)_{I_2}$ and $(\partial W/\partial I_2)_{I_1}$ are not constant, and moreover cannot be determined from uniaxial data alone. It is therefore not possible to interpret the slope and intercept of *Figure 16* in molecular terms. There are however a number of factors (for review see refs 23 and 24) which suggest that the deviations from the simple theory formally represented by the $C_2$ term may be related to local orientational order, as has been suggested by Rehage and coworkers[25], by Boyer[23] and a quantitative treatment attempted by Schwarz[26].

## CONCLUSIONS

The measurements of birefringence shrinkage and shrinkage force on extruded samples of PMMA are consistent with the existence of a molecular network. The development of orientation is dependent on the temperature of deformation, and certain aspects can be very well understood in terms of a different density of crosslink points at different temperatures. It is possible that the crosslinks could be the electrostatic interactions envisaged by Raha and Bowden, together with more permanent physical entanglements which are stable above $T_g$.

The development of birefringence and shrinkage force with strain cannot however be explained on the basis of the

most elementary theories of rubber networks. The alternative of a more sophisticated phenomenological approach (the Mooney–Rivlin equation) has been explored and shown to give a good fit to the data. More detailed studies, particularly of the annealing behaviour, are required before a definitive physical picture can emerge.

## ACKNOWLEDGEMENTS

One of us (N. K.) wishes to thank the British Council for financial support under the Colombo Plan. We would also acknowledge the assistance of Mr T. J. Bednarczyk in compiling the data in *Figure 3*.

## REFERENCES

1 Gibson, A. G., Ward, I. M., Cole, B. N. and Parsons, B. *J. Mater. Sci.* 1974, **9**, 1193
2 Kashiwagi, M., Folkes, M. J. and Ward, I. M. *Polymer* 1971, **12**, 697
3 Purvis, J. and Bower, D. I. *Polymer* 1974, **15**, 645
4 Raha, S. and Bowden, P. B. *Polymer* 1972, **13**, 174
5 Pinnock, P. R. and Ward, I. M. *Trans. Faraday Soc.* 1966, **62**, 1308
6 Shishkin, N. I. and Milagin, M. F. *Sov. Phys. Solid State* 1963, **4**, 1967
7 Kahar, N. *PhD Thesis* University of Leeds (1976)
8 Haward, R. N., Murphy, B. M. and White, E. F. T. in 'Proc. 2nd International Conference on Fracture', (Ed. Pratt), Chapman and Hall, London, 1969, p. 519
9 Kuhn, W. and Grün, F. *Kolloid-Z.* 1942, **101**, 248
10 Cunningham, A., Ward, I. M., Willis, H. A. and Zichy, V. I. *Polymer* 1974, **15**, 749
11 Ward, I. M. *Br. J. Appl. Phys.* 1967, **18**, 1165
12 Ward, I. M. 'The Mechanical Properties of Solid Polymers', Wiley, London, 1971, p. 257
13 Allison, S. M. and Ward, I. M. *Br. J. Appl. Phys.* 1967, **18**, 1151
14 Foot, J. S. and Ward, I. M. *J. Mater. Sci.* 1976, **10**, 955
15 Hibi, S., Maeda, M., Kubota, H. and Miura, T. *Polymer* 1977, **18**, 137
16 Picot, C., Duplessix, R., Decker, D., Benoit, H., Boue, F., Colton, J. P., Pincus, P., Daoud, M., Famoux, B., Janninck, G., Nierlich, M. and de Vries, A. J. *Macromolecules* in press
17 Andrews, R. D. and Hammack, T. J. *J. Polym. Sci. (C)* 1964, **5**, 101
18 Read, B. E. *J. Polym. Sci. (C)* 1967, **16**, 1887
19 Tsvetkov, V. N. and Verkhotina, L. N. *Sov. Phys.–Tech. Phys.* 1958, **3**, 87
20 Hennig, J. *3rd Int. Conf. Amorphous Mater. Clausthal* 1976
21 Treloar, L. R. G. *Proc. Roy. Soc. (London) (A)* 1976, **351**, 301
22 Saunders, D. W. *Trans. Faraday Soc.* 1957, **53**, 860
23 Boyer, R. F. *J. Macromol. Sci. (B)* 1976, **12**, 253
24 Hadley, D. W. and Ward, I. M. *Rep. Prog. Phys.* 1975, **38**, 1143
25 Rehage, G. *Pure Appl. Chem.* 1974, **39**, 161
26 Schwarz, J. *Kolloid Z. Z. Polym.* 1973, **251**